Climatic Responses to Future Trans-Arctic Shipping

Scott R. Stephenson[1] iD, **Wenshan Wang[2]** iD, **Charles S. Zender[2]** iD, **Hailong Wang[3]** iD, **Steven J. Davis[2]** iD, and **Philip J. Rasch[3]** iD

[1]Department of Geography, University of Connecticut, Storrs, CT, USA, [2]Department of Earth System Science, University of California, Irvine, CA, USA, [3]Pacific Northwest National Laboratory, Richland, WA, USA

Abstract As global temperatures increase, sea ice loss will increasingly enable commercial shipping traffic to cross the Arctic Ocean, where the ships' gas and particulate emissions may have strong regional effects. Here we investigate impacts of shipping emissions on Arctic climate using a fully coupled Earth system model (CESM 1.2.2) and a suite of newly developed projections of 21st-century trans-Arctic shipping emissions. We find that trans-Arctic shipping will reduce Arctic warming by nearly 1 °C by 2099, due to sulfate-driven liquid water cloud formation. Cloud fraction and liquid water path exhibit significant positive trends, cooling the lower atmosphere and surface. Positive feedbacks from sea ice growth-induced albedo increases and decreased downwelling longwave radiation due to reduced water vapor content amplify the cooling relative to the shipping-free Arctic. Our findings thus point to the complexity in Arctic climate responses to increased shipping traffic, justifying further study and policy considerations as trade routes open.

Plain Language Summary Global warming is melting Arctic sea ice, thereby enabling greater maritime access to the Arctic Ocean. Emissions such as black carbon and sulfur from ships have the potential to warm the climate further by darkening snow and ice surfaces or cool the climate by promoting cloud formation. This study used a global Earth system model to simulate the climatic effects of emissions from ships crossing the Arctic Ocean from the present to 2099. We find that shipping emissions increase formation of clouds with high liquid water content, and cause the Arctic surface air to cool nearly 1° by 2099 relative to the shipping-free Arctic. This cooling effect was amplified further by sea ice growth and reduced atmospheric water vapor. Our results illustrate the complexity of climatic responses to increased shipping in the Arctic and the need for greater understanding of the reciprocal nature of climate and human activities.

1. Introduction

Younger, thinner, and less-extensive sea ice (Lindsay & Schweiger, 2015; Stroeve et al., 2012) is altering the Arctic climate system (Cohen et al., 2012; Dall'Osto et al., 2017; Semenov et al., 2015; Stroeve et al., 2014; Tang et al., 2013) and enabling human access to more of the Arctic Ocean than ever before (Stephenson, 2017; Stephenson & Pincus, 2018). In particular, the prospect of trans-Arctic shipping is supported by shipping simulations that show robust increases in trans-Arctic access by midcentury under multimodel climate projections (Aksenov et al., 2017; Khon et al., 2017; Melia et al., 2016; Stephenson & Smith, 2015). Of particular geopolitical interest is the so-called *trans-polar route* over the North Pole, the shortest theoretical crossing between the North Atlantic and the Bering Strait that circumvents central Arctic state territorial waters and Exclusive Economic Zones (Clarke-Sather et al., 2017). Although the economic viability of transit shipping along such Arctic routes is still debated (Brigham, 2010; Lasserre, 2015; Meng et al., 2016), ship traffic appears likely to increase in the coming decades due to increasing resource extraction, resupply of growing communities, and tourism (Farré et al., 2014; Yumashev et al., 2017).

Because warming favors increased shipping traffic, previous studies have focused on the potential for ship emissions of black carbon (BC) and other particulates to enhance warming by lowering the otherwise high albedo of ice and snow (Browse et al., 2013; Corbett et al., 2010; Ødemark et al., 2012; Sand et al., 2016). The source of emissions is an important factor in determining the magnitude of this feedback and their ultimate climatic impact. Unlike BC transported to the Arctic from these midlatitude sources in Russia and Asia (Winiger et al., 2017; Wobus et al., 2016), strong surface inversions in the Arctic boundary layer make it more likely that BC emitted in the Arctic will be deposited on ice and snow, thereby maximizing its impact on surface temperature. However, previous studies demonstrated significant warming signals from reduced

albedo only after scaling BC emissions more than 100 times above the current average ambient BC levels in the Arctic (Sand et al., 2013).

Other mechanisms of radiative forcing are also important to Arctic temperatures. The insulating effect of longwave absorption by clouds may amplify Arctic warming (Cox et al., 2015), and Arctic clouds are particularly sensitive to increases in cloud condensation nuclei (CCN) from pollution due to the stability of Arctic air masses (Coopman et al., 2018). In opposition, emissions of sulfur oxides (SO_2) and resulting sulfate (SO_4) generate a direct negative radiative forcing by scattering incoming sunlight (Charlson et al., 1992), which may offset a significant part of the BC heating effect in the Arctic (Yang et al., 2018). Lastly, an increase in atmospheric particulates that serve as CCN will tend to increase cloud albedo by encouraging formation of smaller and more numerous cloud droplets (Twomey, 1977), particularly in liquid clouds (Christensen et al., 2014; Morrison et al., 2012). Although the influence of particulate emissions in the Arctic has historically been small and localized relative to more populous lower latitudes (Gong et al., 2018; Peters et al., 2011), increases in shipping emissions could substantially raise CCN, enhance cloud formation, and induce a climatic response (Mueller, 2018; Wang et al., 2013; Yang et al., 2018).

Previous studies have investigated the interacting effects of short-lived pollutants from Arctic shipping scenarios with mixed and contrasting results. Using chemical transport and radiative forcing models, Dalsøren et al. (2013) found warming under two spatially explicit emission scenarios (Peters et al., 2011) between 2004 and 2030, while Fuglestvedt et al. (2014) used a simple 2-box climate model to demonstrate enhanced Arctic warming from short-lived shipping pollutants until 2160. In contrast, Gilgen et al. (2017) found net cooling by 2050 using a global aerosol-climate model, driven by enhanced cloud droplet number and optical thickness of clouds over the Arctic Ocean. Although highly relevant to environmental impacts of future shipping, the methods and emission projections used previously are not capable of evaluating dynamic feedbacks in the physical climate and human activities. We build on these earlier studies by using a fully coupled Earth system model (ESM) forced by spatially and temporally explicit projections of trans-Arctic shipping emissions between 2006 and 2099. Unlike previous studies, this ESM simulates the physical interactions of albedo, clouds, oceans, and sea ice, and the emission projections employed allow specific shipping routes to vary with seasonal and decadal changes in sea ice so that shipping routes span multiple marine pathways (e.g., the coastal Northern Sea Route and direct transits over the North Pole). Our results thus represent a more realistic and robust estimate of climate responses to future trans-Arctic shipping.

2. Methods

2.1. Trans-Arctic Shipping Emissions

Projected emission inventories from trans-Arctic shipping during the period 2006–2099 were derived from simulated voyages computed by combining ESM-projected sea ice distribution with projected Europe-Asia trade. Transits take place when two conditions are met: (1) sea ice conditions enable technical access between Europe and Asia; (2) operating costs of shipping via the least-cost Arctic route are lower than via the Suez Canal route. Full details are given in supporting information.

2.1.1. Technical Shipping Access

The methodology for calculating technical shipping access extends the approach of Stephenson and Smith (2015). Monthly projected sea ice concentration and thickness data are obtained from 10 ESMs shown to simulate well the observed climatology, trend, and seasonal amplitude of 20th-century and early 21st-century sea ice extent and volume (Jahn et al., 2012; J. Liu et al., 2013; Massonnet et al., 2012; Stephenson & Smith, 2015). Monthly data are averaged across models to form the ensemble average of sea ice concentration and thickness from 2006 to 2099. Optimal least-cost navigation routes are derived from ESM data following the Arctic Ice Regime Shipping System framework (Transport Canada, 1998) described in detail by Stephenson et al. (2013). Pairwise Europe-Asia routes are computed using a least-cost path algorithm between 4 European and 14 East Asian port regions (combining ports serving common regional markets) that are among the top 50 ports worldwide in 2010 *twenty-foot equivalent unit* traffic (Containerisation International, 2012). Route paths are allowed to vary to minimize transit time, encompassing coastal routes such as the Northern Sea Route and Northwest Passage as well as direct transits over the North Pole.

AGU
100
ADVANCING EARTH
AND SPACE SCIENCE

Geophysical Research Letters

10.1029/2018GL078969

2.1.2. Shipping Emissions

In addition to technical accessibility, Arctic routes require a cost incentive to justify their use over the traditional Suez Canal route. A cost incentive is assumed when the cost of transporting a unit of cargo via the Arctic is lower than via the Suez Canal. Owing to beam and draft limitations along the Northern Sea Route (Brigham et al., 1999), a standard Panamax vessel (80,000 deadweight tons [dwt] capacity) is assumed for Arctic transits, while a larger *New Panamax* (120,000 dwt capacity) is assumed for Suez transits (Stott, 2012). Ships are assumed to operate at full capacity. The transport cost per unit of cargo (2010 dollars) via the Arctic is calculated as:

$$D_A * F_A * P * E * G / C_A,$$

where D_A is the voyage time, F_A is the fuel consumption rate, P is the bunker fuel price, E is a fuel consumption scaling factor based on the Energy Efficient Design Index, G is a scaling factor accounting for global GDP increase, and C_A is the cargo capacity (metric tons). The transport cost per unit of cargo via the Suez Canal is calculated in a similar way:

$$(D_S * F_S * P * E + T) * G / C_S,$$

where D_S, F_S, and C_S represent voyage time via the Suez Canal (SeaRates, 2016), fuel consumption rate for a New Panamax vessel (516 metric tons per day; AECOM, 2012), and cargo capacity for a New Panamax vessel, respectively, and T is the Suez Canal transit fee (Suez Canal Authority, 2010). When transport cost is lower via the Suez Canal than via the Arctic for a given month, no Arctic transit is projected to take place.

Emissions from Arctic shipping in a given month are derived from the aggregate fuel consumption of Arctic transits, determined from the number of fully laden transits (rounded up) using an 80,000-dwt vessel that would be required to transport the quantity of traded goods projected for each Europe-Asia port pair in a given month. Aggregate fuel consumption is calculated by multiplying the fuel consumption per transit by the number of required transits for each port pair, then summing for all port pairs. Gridded fuel consumption is estimated by distributing the aggregate quantity of fuel consumed over the least-cost routes determined in section 2.1.1, weighted by the number of vessels passing through the grid cell. Gridded fuel consumption is converted to emissions of BC, OC, and SO_2 based on emissions factors described by Buhaug et al. (2009) and Corbett et al. (2010).

2.2. The Community Earth System Model

To investigate climate responses to the projected trans-Arctic shipping emissions, we use the latest version (1.2.2) of the Community Earth System Model (CESM) from the National Center for Atmospheric Research (Hurrell et al., 2013). CESM is a fully coupled global climate model that provides the state-of-the-art simulations of climate states without any *flux adjustment*. It consists of atmosphere (Community Atmosphere Model, CAM5), land (Community Land Model, CLM4.0 including Carbon and Nitrogen cycles), ocean (Parallel Ocean Program, POP2), and sea ice (Los Alamos Sea Ice Model, CICE) components at 1° resolution.

Estimated monthly trans-Arctic shipping emissions (BC, OC, SO_2, and SO_4) are injected into the lowest atmospheric model layer along with other emission inventories from IPCC AR5 (Lamarque et al., 2010) under the RCP 8.5 scenario. BC, OC, and SO_4 from shipping emissions are injected in the accumulation mode (between 0.1 and 2.5 μm). SO_4 from shipping is estimated as 2.5% of SO_2, consistent with other emission inventories from IPCC AR5, while the remaining 97.5% of SO_2 is injected to the bottom layer of the model and eventually converts to SO_4 in different size modes through a series of chemical and aerosol microphysical processes (X. Liu et al., 2012). Following one spin-up year (2005) branched from a 20th-century transient climate simulation, we simulate and analyze the period 2006–2099. The 2005 spin-up year allows atmospheric processes at local to regional scales to equilibrate to initial aerosol forcing (Simmonds, 1985), after which seasonal trans-Arctic shipping emissions increase (Figure 1b). Five ensemble runs with slight perturbations in their initial temperatures comprise the experiment. Results are compared to a 40-member average of control simulations from the CESM Large Ensemble Project (LENS), an ensemble of fully coupled CESM1 simulations under RCP 8.5 (Kay et al., 2015). A control run using the same model version and component set as the experiment
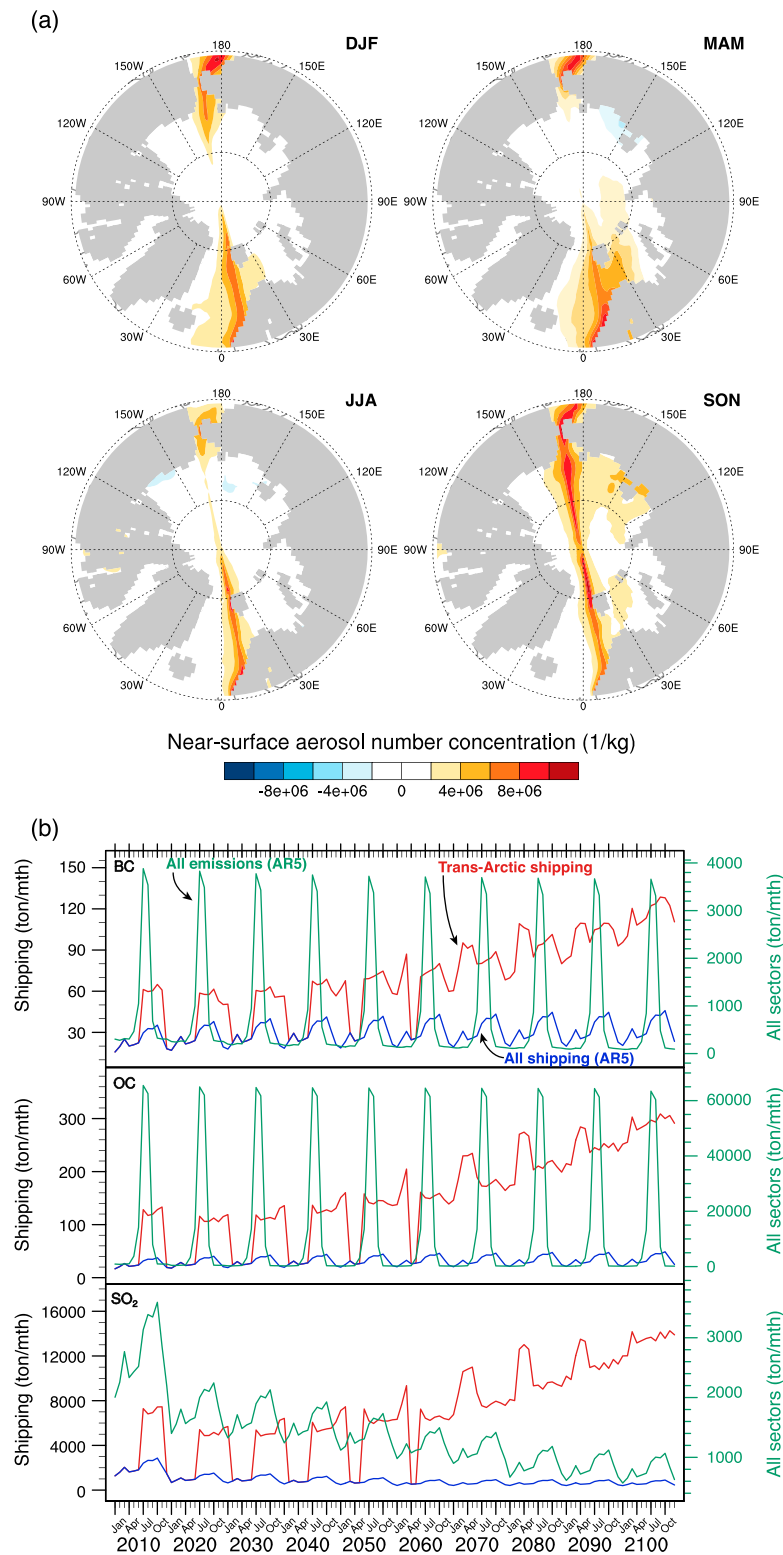
Figure 1. (a) Difference in near-surface accumulation mode aerosol number concentration averaged from 2070 to 2099 (experiment minus LENS control); (b) black carbon, OC, and SO_2 emissions north of 66.5°N from trans-Arctic shipping (red curves; SO_4 calculated as 2.5% of SO_2 at the surface) added to experiment runs, along with black carbon, OC and SO_2 loadings from shipping in IPCC AR5 (blue curves) and from all sources in IPCC AR5 (green curves) in experiment and LENS control runs. Emissions are shown as monthly means for every 10 years (2010, 2020, …, 2100) and linearly interpolated in years between in model simulations. DJF = December-January-February; MAM = March-April-May; JJA = June-July-August; SON = September-October-November.
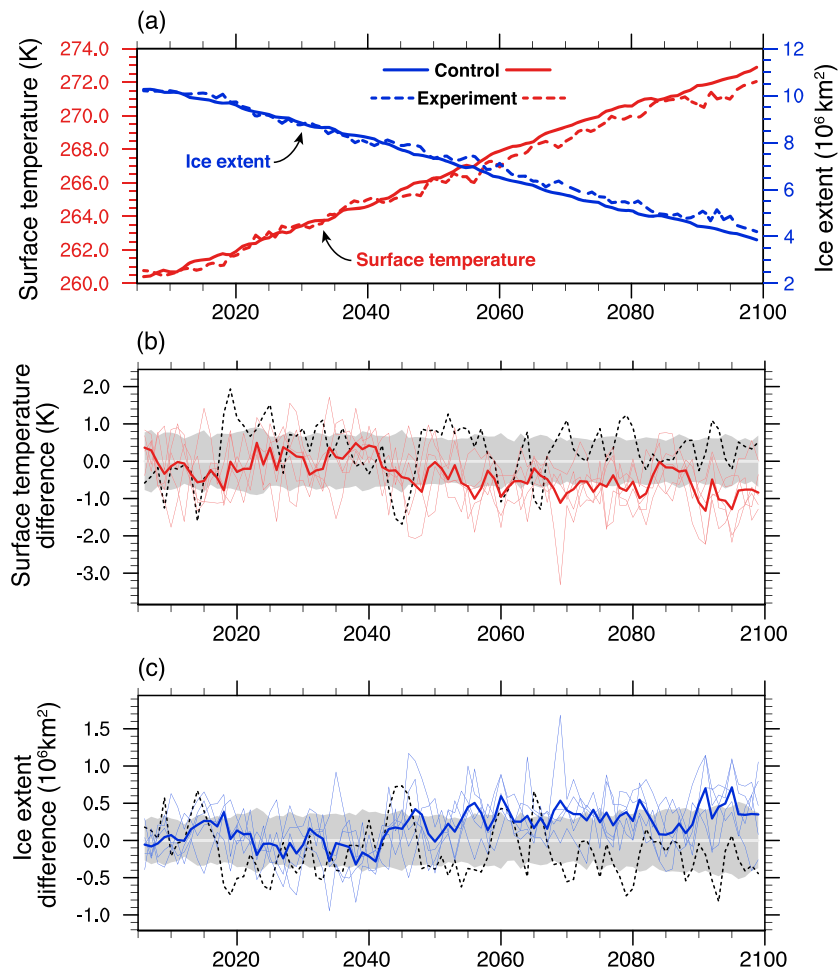
Figure 2. Multidecadal change in (a) sea surface temperature and sea ice extent; (b) sea surface temperature difference (experiment minus LENS control); (c) sea ice extent difference (experiment minus LENS control) north of 66.5°N, with a Community Earth System Model (CAM 5.3) control run shown for reference (dotted lines). Gray areas indicate one standard deviation of the 40-member LENS ensemble.

was also performed for comparison with LENS simulations. Except for trans-Arctic shipping emissions, external forcing in the experiment runs is identical to that of the LENS ensemble.

Results are analyzed for the ocean region north of 66.5°N. Figure 1 shows (a) the difference in near-surface aerosol number concentration in the accumulation mode averaged from 2070 to 2099 between the experiment runs and LENS ensemble-average control runs and (b) added trans-Arctic shipping emissions and emissions from nonshipping sources. Near-surface averages rather than whole-column averages are shown in order to clearly illustrate aerosol distributions added to the model along shipping tracks at the surface. By 2070, most optimal trans-Arctic routes pass over the North Pole rather than along the coastal NSR, leading to the accumulation pattern shown in Figure 1a.

3. Results

Our experiment demonstrates a clear and small yet significant slowing of Arctic warming as a result of trans-Arctic shipping emissions. Figure 2 shows that by 2099, sea surface temperature (SST) north of 66.5°N is nearly 1 °C cooler, and sea ice extent greater by nearly 500,000 km^2, in the experiment runs compared to the LENS control. The shipping-induced cooling (~1 °C) is a small fraction of net RCP8.5 warming (~10 °C), comparable in magnitude (though opposite in sign) to Arctic warming from anthropogenic CH_4 scaled to the LENS control results over the same period, based on CH_4 effective radiative forcing (IPCC, 2013).

Patterns of relative cooling vary spatially and seasonally. The greatest cooling and sea ice growth occur throughout the central Arctic basin in winter (DJF) and along the Greenland-Barents Sea ice edge in spring (MAM; Figure 3). This seasonal pattern is driven mainly by the ice-ocean contrast, as new sea ice depresses surface temperature due to reduced ocean-atmosphere heat exchange and increased albedo (Ruddiman, 2001). Cooling occurs throughout the Arctic rather than along the ocean swaths corresponding to least-cost shipping routes, indicating that climatic impacts from shipping will be regional rather than local in scale. Cooling is most significant from 2060 onward due to a step change in emissions in late winter/early spring, owing to a 613% increase in shipping transits in MAM from 2060 to 2099 compared with a 143% increase during the rest of the year over this period. Period-averaged differences in key climatic variables between experiment and control runs, with significance indicators from a two-tailed Student's t test, are in Table S1.

Cooling trends in the experiment are underpinned by robust increases in cloud cover and liquid water content, primarily along shipping routes, driven by sulfate (SO_4) aerosol enhancement. Figure S1 depicts increases in total cloud fraction of over 0.3% per year and in cloud liquid water path of over 0.3 g/m^2 per year from 2006 to 2099 in the experiment runs, leading to cumulative increases of approximately 35% and 5 g/m^2, respectively, by 2099. The experimental cloud fraction and cloud liquid water path substantially exceed one standard deviation beyond their LENS control counterparts. Cloud fraction increases are widespread over the central Arctic Ocean in spring (MAM) and summer (JJA), while liquid water path increases are primarily in summer (Figure S2). Cloud fraction and water (both ice and liquid) changes are negligible during winter (DJF) despite the largest changes in temperature and ice concentration occurring in this season (Figure 3). This winter temperature decrease is a *delayed cooling* that stems from a sharp decrease in radiative flux in summer (Figure S7a) which lowers SST over open water in fall (Figure S7b) and enhances ice growth in winter (Figure S7c). More relatively warm ocean area covered by sea ice causes a marked temperature decrease throughout the Arctic basin in the experiment runs compared to the LENS control (Figure S7b). A snapshot in 2099 shows close spatial correspondence between surface temperature and ice fraction (Figure S8). Winter sea ice growth also insulates water beneath the ice, decreasing turbulent heat release to the atmosphere (Figure S7a), thus increasing winter SST (Figure S7b). This delayed cooling is the reverse of the *delayed warming* associated with Arctic amplification as described by Screen and Simmonds (2010), by which an energy surplus in summer elevates SST in fall, enhancing warming throughout the Arctic basin in winter.

Surface and atmosphere radiation fluxes and cloud radiative effects reveal the pathways through which shipping-induced cooling occurs. Rather than clouds cooling the surface directly, surface cooling occurs via sensible heat transfer from the surface to the outgoing longwave-cooled lower atmosphere. Increased downwelling longwave radiation from clouds approximately balances reduced surface insolation due to cloud albedo, causing the annual mean net cloud radiative effect at the surface to be small and insignificant (Figure S3; Table S1). These surface cloud radiative effects are strongly seasonal, with peak warming in May, when higher surface albedo from remaining sea ice in spring reduces cloud shading effects so cloud longwave heating dominates, followed by cooling in July, when cloud shading of the surface outweighs cloud longwave heating (Figure S4). Instead, clouds cool the lower atmosphere through enhanced longwave outgoing radiation. Simulated trans-Arctic shipping increases cloud fraction (Figure 4a) and liquid water content (Figure 4b) mainly in the lower atmosphere below 850 hPa in response to low-altitude CCN enhancement by ship emissions. Outside the tropics, clouds typically cool the atmosphere in the longwave because cloud top emission exceeds cloud base warming, while shortwave cloud absorption always warms the atmosphere (Wallace & Hobbs, 2006). Relative to the control, our experiment exhibits both longwave cooling (Figure 4c) and shortwave warming (Figure 4d) of the lower atmosphere, with net radiative loss (Figure 4e) and temperature decrease (Figure 4f) indicating greater longwave than shortwave effects. This cooling in the lower atmosphere is more likely caused by liquid cloud enhancement than water vapor or ice clouds because the atmospheric column is drier in the experiment owing to temperature reduction (Figure 4g) and the ice water path is low (<10 g/m^2) and changes much less than the liquid water path in the experiment. This energy loss in the lower atmosphere is then mediated by sensible heat transfer from the surface (Figure S5). The sensible heat transfer promotes further surface cooling through two positive feedbacks: (1) the ice-albedo effect further reducing absorbed shortwave radiation; (2) lower water vapor content reducing downwelling longwave radiation to the surface. While lower water vapor enables more
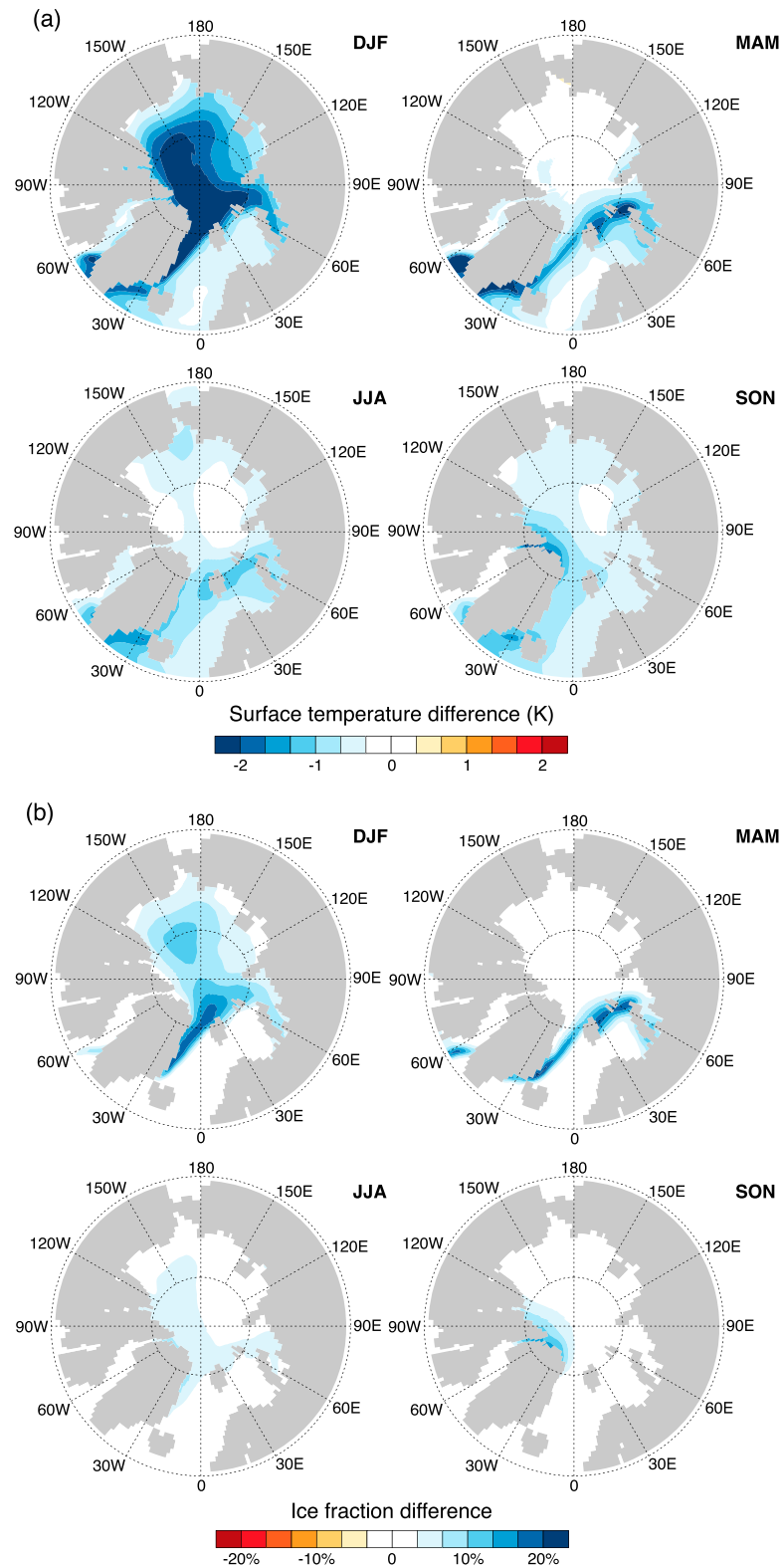
Figure 3. Seasonal average (2070–2099) of difference in (a) surface temperature and (b) sea ice fraction (experiment minus LENS control). DJF = December-January-February; MAM = March-April-May; JJA = June-July-August; SON = September-October-November.
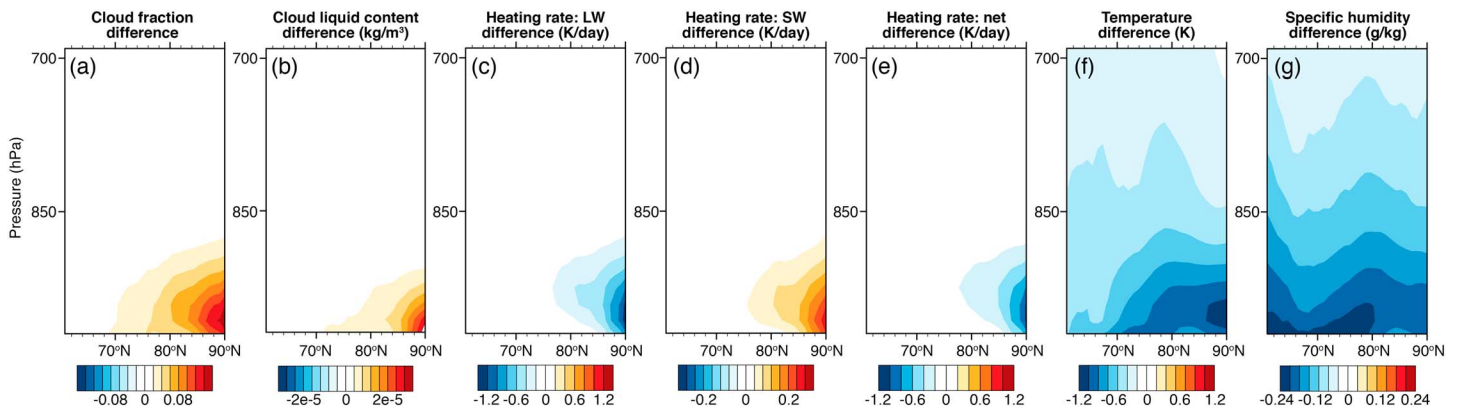
Figure 4. Meridional (*x* axis; 60–90°N) and pressure (*y* axis; 700–1,000 hPa) profiles of May–September difference in (a) cloud fraction; (b) liquid water content; (c) longwave heating rate; (d) shortwave heating rate; (e) net heating rate; (f) temperature; and (g) specific humidity (2070–2099 average; experiment minus LENS control).

shortwave radiation to reach the lower atmosphere (Figure 4d), its greater impact is to reduce the atmospheric absorption of outgoing longwave radiation, allowing net cooling. The net radiative loss from clouds and the attendant ice-albedo and water vapor feedbacks at the surface in the experiment runs is illustrated in Figure S6. The longwave radiation trend is positive, driven by downwelling from clouds and mediated by reduced water vapor at the surface, while shortwave radiation is more strongly negative, driven by liquid-enhanced cloud reflectance and increased surface albedo. The overall effect is the significant surface cooling in the latter half of the 21st century.

4. Discussion and Conclusions

Our simulations assume a future of continued overall Arctic ice decline, growing global economic output, and sustained (though not necessarily increasing) integration of Asian and European markets in line with IPCC high-emissions scenario assumptions (Riahi et al., 2011). However, even as the Arctic continues to warm at twice the rate of the global average, we find that the net regional climatic impact of trans-Arctic shipping emissions will likely be less warming. This is because in contrast to previous studies, increased BC emissions do not cause significant warming in our simulations relative to cloud radiative effects, in line with minor BC radiative forcing found in the Arctic from in situ measurements (0.06 W/m^2) and previous model simulations (0.51 W/m^2; Dang et al., 2017; Qian et al., 2014). Instead, aerosol direct effects are offset by reduced water vapor enabling increased shortwave downwelling and reduced surface albedo from BC is counteracted by substantial increases in cloud albedo. In short, cooling driven by sulfate-induced liquid cloud formation dominates in our experiment. However, we emphasize that the magnitude of this cooling effect (~1 °C) is roughly an order of magnitude smaller than the overall regional warming in RCP 8.5 (~10 °C). Although the CESM model that we use is more sophisticated than those used in prior studies, it is possible that the cooling we simulate may reflect enhanced liquid water path caused by a large decrease in the rate of conversion of cloud to rainwater when cloud droplet number increases (Wang et al., 2013; Zhou & Penner, 2017). The current atmospheric component of CESM (CAM5) has a more realistic representation of cloud properties than its predecessor (CAM4), with a substantial improvement in Arctic cloud seasonal cycle (Kay et al., 2012). CAM5 has been shown to underestimate cloud liquid water path and ice water path in the Arctic relative to observations (Komurcu et al., 2014), though to a lesser degree than other CMIP5 models. Further improvements in the representation of cloud-aerosol physics in ESMs will be necessary to confirm or alter our conclusions and further reduce uncertainty in climate projections (Schneider et al., 2017).

Our results should not be taken as an endorsement of Arctic shipping as a solution to climate change. In addition to enhancing the risk of oil spills in ice-covered waters, shipping enables extraction of new Arctic hydrocarbon resources, accelerating warming and delaying the transition toward a low-carbon energy system. For example, investment in ice-class carriers is often cited as a prerequisite for further development of Russian Arctic oil, gas, and mineral projects along the Northern Sea Route, such as Yamal LNG and Norilsk

Nickel (Orttung & Reisser, 2014; Stephenson & Agnew, 2016). As shipping will likely contribute a minor share of the total Arctic aerosol emissions by midcentury (Browse et al., 2013), BC from such coastal sources may counteract the cooling effect from enhanced clouds. Furthermore, planned global limits on ships' SO_2 emissions after 2020 (IMO, 2018) will reduce aerosol cooling from shipping in much the same way that air quality improvements since the 1970s have unmasked GHG warming in urban areas. In this way, the net climatic impact of Arctic shipping will ultimately depend on international regulatory and trade agreements in addition to marine access. Our results thus highlight a need for integrated analysis of climatic and transport systems to further clarify the reciprocal relationship of climate and human activities in the Arctic.

References

AECOM (2012). North Carolina Maritime Strategy: Vessel Size vs. Cost. North Carolina Department of Transportation. Raleigh.

Aksenov, Y., Popova, E., Yool, A., Nurser, A. J. G., Williams, T. D., Bertino, L., & Bergh, J. (2017). On the future navigability of Arctic sea routes: High-resolution projections of the Arctic Ocean and sea ice. *Marine Policy*, 75, 300–317. https://doi.org/10.1016/j.marpol.2015.12.027i

Brigham, L.W. (2010). Think again: The Arctic. Foreign Policy

Brigham, L. W., Grishchenko, V. D., & Kamisaki, K. (1999). The natural environment, ice navigation and ship technology. In W. Østreng (Ed.), *The natural and societal challenges of the Northern Sea Route* (pp. 47–120). London: Kluwer Academic Publishers. https://doi.org/10.1007/978-94-015-9409-7_2

Browse, J., Carslaw, K. S., Schmidt, A., & Corbett, J. J. (2013). Impact of future Arctic shipping on high-latitude black carbon deposition. *Geophysical Research Letters*, 40, 4459–4463. https://doi.org/10.1002/grl.50876

Buhaug, Ø., JJ. Corbett, Ø. Endresen, V. Eyring, J. Faber, S. Hanayama, et al. (2009). Second IMO greenhouse gas study 2009. International Maritime Organization. London.

Charlson, R. J., Schwartz, S. E., Hales, J. M., Cess, R. D., Coakley, J. A., Hansen, J. E., & Hofmann, D. J. (1992). Climate forcing by anthropogenic aerosols. *Science*, 24, 423–430.

Christensen, M. W., Suzuki, K., Zambri, B., & Stephens, G. L. (2014). Ship track observations of a reduced shortwave aerosol indirect effect in mixed-phase clouds. *Geophysical Research Letters*, 41, 6970–6977. https://doi.org/10.1002/2014GL061320

Clarke-Sather, A., Crow-Miller, B., Banister, J. M., Thomas, K. A., Norman, E. S., & Stephenson, S. R. (2017). The shifting geopolitics of water in the Anthropocene. *Geopolitics*, 22(2), 332–359. https://doi.org/10.1080/14650045.2017.1282279

Cohen, J. L., Furtado, J. C., Barlow, M. A., Alexeev, V. A., & Cherry, J. E. (2012). Arctic warming, increasing snow cover and widespread boreal winter cooling. *Environmental Research Letters*, 7(1), 014007. https://doi.org/10.1088/1748-9326/7/1/014007

Containerisation International (2012). *Containerisation international yearbook 2012*. London: Informa UK.

Coopman, Q., Garrett, T. J., Finch, D. P., & Riedi, J. (2018). High sensitivity of Arctic liquid clouds to long-range anthropogenic aerosol transport. *Geophysical Research Letters*, 45, 372–381. https://doi.org/10.1002/2017GL075795

Corbett, J. J., Lack, D. A., Winebrake, J. J., Harder, S., Silberman, J. A., & Gold, M. (2010). Arctic shipping emissions inventories and future scenarios. *Atmospheric Chemistry and Physics*, 10(19), 9689–9704. https://doi.org/10.5194/acp-10-9689-2010

Cox, C. J., Walden, V. P., Rowe, P. M., & Shupe, M. D. (2015). Humidity trends imply increased sensitivity to clouds in a warming Arctic. *Nature Communications*, 6(1), 10117. https://doi.org/10.1038/ncomms10117

Dall'Osto, M., Beddows, D. C. S., Tunved, P., Krejci, R., Ström, J., Hansson, H.-C., et al. (2017). Arctic sea ice melt leads to atmospheric new particle formation. *Scientific Reports*, 7(1), 3318. https://doi.org/10.1038/s41598-017-03328-1

Dalsøren, S. B., Samset, B. H., Myhre, G., Corbett, J. J., Minjares, R., Lack, D., & Fuglestvedt, J. S. (2013). Environmental impacts of shipping in 2030 with a particular focus on the Arctic region. *Atmospheric Chemistry and Physics*, 13(4), 1941–1955. https://doi.org/10.5194/acp-13-1941-2013

Dang, C., Warren, S. G., Fu, Q., Doherty, S. J., Sturm, M., & Su, J. (2017). Measurements of light-absorbing particles in snow across the Arctic, North America, and China: Effects on surface albedo. *Journal of Geophysical Research: Atmospheres*, 122, 10149–110168. https://doi.org/10.1002/2017JD027070

Farré, A. B., Stephenson, S. R., Chen, L., Czub, M., Dai, Y., Demchev, D., et al. (2014). Commercial Arctic shipping through the Northeast Passage: Routes, resources, governance, technology, and infrastructure. *Polar Geography*, 37(4), 298–324. https://doi.org/10.1080/1088937X.2014.965769

Fuglestvedt, J. S., Dalsøren, S. B., Samset, B. H., Berntsen, T. K., Myhre, G., Hodnebrog, Ø., et al. (2014). Climate penalty for shifting shipping to the Arctic. *Environmental Science and Technology*, 48(22), 13,273–13,279. https://doi.org/10.1021/es502379d

Gilgen, A., Huang, W. T. K., Ickes, L., Neubauer, D., & Lohmann, U. (2017). How important are future marine and shipping aerosol emissions in warming Arctic summer and autumn? *Atmospheric Chemistry and Physics Discussions*, 1–41. https://doi.org/10.5194/acp-2017-1007

Gong, W., Beagley, S. R., Cousineau, S., Sassi, M., Munoz-Alpizar, R., Menard, S., et al. (2018). Assessing the impact of shipping emissions on air pollution in the Canadian Arctic and northern regions: Current and future modelled scenarios. *Atmospheric Chemistry and Physics Discussions*, 1–54. https://doi.org/10.5194/acp-2018-125

Hurrell, J. W., Holland, M. M., Gent, P. R., Ghan, S., Kay, J. E., Kushner, P. J., et al. (2013). The Community Earth System Model: A framework for collaborative research. *Bulletin of the American Meteorological Society*, 94(9), 1339–1360. https://doi.org/10.1175/BAMS-D-12-00121.1

IMO (2018). The 2020 global sulphur limit. International Maritime Organization. Retrieved from http://www.imo.org/en/MediaCentre/HotTopics/GHG/Documents/FAQ_2020_English.pdf

IPCC (2013). Annex II: Climate system scenario tables [Prather, M., G. Flato, P. Friedlingstein, C. Jones, J.-F. Lamarque, H. Liao and P. Rasch (eds.)]. In T. F. Stocker, et al. (Eds.), *Climate change 2013: The physical science basis. Contribution of working group I to the fifth assessment report of the intergovernmental panel on climate change* (pp. 1395–1445). Cambridge, UK: Cambridge University Press.

Jahn, A., Sterling, K., Holland, M. M., Kay, J. E., Maslanik, J. A., Bitz, C. M., et al. (2012). Late-twentieth-century simulation of Arctic sea ice and ocean properties in the CCSM4. *Journal of Climate*, 25(5), 1431–1452. https://doi.org/10.1175/JCLI-D-11-00201.1

Kay, J. E., Deser, C., Phillips, A., Mai, A., Hannay, C., Strand, G., et al. (2015). The Community Earth System Model (CESM) Large Ensemble Project: A community resource for studying climate change in the presence of internal climate variability. *Bulletin of the American Meteorological Society*, 96(8), 1333–1349. https://doi.org/10.1175/BAMS-D-13-00255.1

Kay, J. E., Hillman, B. R., Klein, S. A., Zhang, Y., Medeiros, B., Pincus, R., et al. (2012). Exposing global cloud biases in the Community Atmosphere Model (CAM) using satellite observations and their corresponding instrument simulators. *Journal of Climate*, *25*(15), 5190–5207. https://doi.org/10.1175/JCLI-D-11-00469.1

Khon, V., Mokhov, I., & Semenov, V. (2017). Transit navigation through Northern Sea Route from satellite data and CMIP5 simulations. *Environmental Research Letters*, *12*(2), 024010. https://doi.org/10.1088/1748-9326/aa5841

Komurcu, M., Storelvmo, T., Tan, I., Lohmann, U., Yun, Y., Penner, J. E., et al. (2014). Intercomparison of the cloud water phase among global climate models. *Journal of Geophysical Research: Atmospheres*, *119*, 3372–3400. https://doi.org/10.1002/2013JD021119

Lamarque, J. F., Bond, T. C., Eyring, V., Granier, C., Heil, a., Klimont, Z., et al. (2010). Historical (1850–2000) gridded anthropogenic and biomass burning emissions of reactive gases and aerosols: Methodology and application. *Atmospheric Chemistry and Physics*, *10*(15), 7017–7039. https://doi.org/10.5194/acp-10-7017-2010

Lasserre, F. (2015). Simulations of shipping along Arctic routes: Comparison, analysis and economic perspectives. *Polar Record*, *51*(03), 239–259. https://doi.org/10.1017/S0032247413000958

Lindsay, R., & Schweiger, A. (2015). Arctic sea ice thickness loss determined using subsurface, aircraft, and satellite observations. *The Cryosphere*, *9*(1), 269–283. https://doi.org/10.5194/tc-9-269-2015

Liu, J., Song, M., Horton, R. M., & Hu, Y. (2013). Reducing spread in climate model projections of a September ice-free Arctic. *Proceedings of the National Academy of Sciences*, *110*(31), 12,571–12,576. https://doi.org/10.1073/pnas.1219716110

Liu, X., Easter, R. C., Ghan, S. J., Zaveri, R., Rasch, P., Shi, X. L., et al. (2012). Toward a minimal representation of aerosols in climate models: Description and evaluation in the Community Atmosphere Model CAM5. *Geoscientific Model Development*, *5*(3), 709–739. https://doi.org/10.5194/gmd-5-709-2012

Massonnet, F., Fichefet, T., Goosse, H., Bitz, C. M., Philippon-Berthier, G., Holland, M. M., & Barriat, P.-Y. (2012). Constraining projections of summer Arctic sea ice. *The Cryosphere*, *6*(6), 1383–1394. https://doi.org/10.5194/tc-6-1383-2012

Melia, N., Haines, K., & Hawkins, E. (2016). Sea ice decline and 21st century trans-Arctic shipping routes. *Geophysical Research Letters*, *43*, 9720–9728. https://doi.org/10.1002/2016GL069315

Meng, Q., Zhang, Y., & Xu, M. (2016). Viability of transarctic shipping routes: A literature review from the navigational and commercial perspectives. *Maritime Policy & Management*, *44*, 16–41.

Morrison, H., de Boer, G., Feingold, G., Harrington, J., Shupe, M. D., & Sulia, K. (2012). Resilience of persistent Arctic mixed-phase clouds. *Nature Geoscience*, *5*(1), 11–17. https://doi.org/10.1038/ngeo1332

Mueller, B. L. (2018). Attribution of Arctic sea ice decline from 1953 to 2012 to influences from natural, greenhouse-gas and anthropogenic aerosol forcing. *Journal of Climate*, *31*(19), 7771–7787. https://doi.org/10.1175/JCLI-D-17-0552.1

Ødemark, K., Dalsøren, S. B., Samset, B. H., Berntsen, T. K., Fuglestvedt, J. S., & Myhre, G. (2012). Short-lived climate forcers from current shipping and petroleum activities in the Arctic. *Atmospheric Chemistry and Physics*, *12*(4), 1979–1993. https://doi.org/10.5194/acp-12-1979-2012

Orttung, R. W., & Reisser, C. (2014). Urban sustainability in Russia's Arctic: Lessons from a recent conference and areas for further investigations. *Polar Geography*, *37*(3), 193–214. https://doi.org/10.1080/1088937X.2014.919362

Peters, G. P., Nilssen, T. B., Lindholt, L., Eide, M. S., Glomsrod, S., Eide, L. I., & Fuglestvedt, J. S. (2011). Future emissions from shipping and petroleum activities in the Arctic. *Atmospheric Chemistry and Physics*, *11*(11), 5305–5320. https://doi.org/10.5194/acp-11-5305-2011

Qian, Y., Wang, H., Zhang, R., Flanner, M. G., & Rasch, P. J. (2014). A sensitivity study on modeling black carbon in snow and its radiative forcing over the Arctic and northern China. *Environmental Research Letters*, *9*(6), 064001. https://doi.org/10.1088/1748-9326/9/6/064001

Riahi, K., Rao, S., Krey, V., Cho, C., Chirkov, V., Fischer, G., et al. (2011). RCP 8.5—A scenario of comparatively high greenhouse gas emissions. *Climatic Change*, *109*(1-2), 33–57. https://doi.org/10.1007/s10584-011-0149-y

Ruddiman, W. F. (2001). *Earth's climate: Past and future*. New York: W.H. Freeman & Co.

Sand, M., Berntsen, T. K., Seland, Ø., & Kristjánsson, J. E. (2013). Arctic surface temperature change to emissions of black carbon within Arctic or midlatitudes. *Journal of Geophysical Research: Atmospheres*, *118*, 7788–7798. https://doi.org/10.1002/jgrd.50613

Sand, M., Berntsen, T. K., von Salzen, K., Flanner, M. G., Langner, J., & Victor, D. G. (2016). Response of Arctic temperature to changes in emissions of short-lived climate forcers. *Nature Climate Change*, *6*(3), 286–289. https://doi.org/10.1038/NCLIMATE2880

Schneider, T., Teixeira, J., Bretherton, C. S., Brient, F., Pressel, K. G., Schär, C., & Siebesma, A. P. (2017). Climate goals and computing the future of clouds. *Nature Climate Change*, *7*(1), 3–5. https://doi.org/10.1038/nclimate3190

Screen, J. A., & Simmonds, I. (2010). Increasing fall-winter energy loss from the Arctic Ocean and its role in Arctic temperature amplification. *Geophysical Research Letters*, *37*(16), L16707. https://doi.org/10.1029/2010GL044136

SeaRates (2016). Port distances and time. Retrieved from https://www.searates.com/reference/portdistance

Semenov, V. A., Martin, T., Behrens, L. K., & Latif, M. (2015). Arctic sea ice area in CMIP3 and CMIP5 climate model ensembles – Variability and change. *The Cryosphere Discussions*, *9*(1), 1077–1131. https://doi.org/10.5194/tcd-9-1077-2015

Simmonds, I. (1985). Analysis of the "spinup" of a general circulation model. *Journal of Geophysical Research*, *90*, 5637–5660. https://doi.org/10.1029/JD090iD03p05637

Stephenson, S. R. (2017). Access to Arctic urban areas in flux: Opportunities and uncertainties in transport and development. In R. Orttung (Ed.), *Sustaining Russia's Arctic cities: Resource politics, migration, and climate change* (pp. 175–200). New York: Berghahn.

Stephenson, S. R., & Agnew, J. A. (2016). The work of networks: Embedding firms, transport, and the state in the Russian Arctic oil and gas sector. *Environment and Planning A*, *48*(3), 558–576. https://doi.org/10.1177/0308518X15617755

Stephenson, S. R., & Pincus, R. (2018). Challenges of sea-ice prediction for Arctic marine policy and planning. *Journal of Borderlands Studies*, *33*(2), 255–272. https://doi.org/10.1080/08865655.2017.1294494

Stephenson, S. R., & Smith, L. C. (2015). Influence of climate model variability on projected Arctic shipping futures. *Earth's Future*, *3*(11), 331–343. https://doi.org/10.1002/2015EF000317

Stephenson, S. R., Smith, L. C., Brigham, L. W., & Agnew, J. A. (2013). Projected 21st-century changes to Arctic marine access. *Climatic Change*, *118*(3-4), 885–899. https://doi.org/10.1007/s10584-012-0685-0

Stott, P. W. (2012). New Panamax and its implications for ship design and efficiency. Low Carbon Shipping Conference 2012, Newcastle University.

Stroeve, J. C., Kattsov, V., Barrett, A., Serreze, M., Pavlova, T., Holland, M., & Meier, W. N. (2012). Trends in Arctic sea ice extent from CMIP5, CMIP3 and observations. *Geophysical Research Letters*, *39*, L16502. https://doi.org/10.1029/2012GL052676

Stroeve, J. C., Markus, T., Boisvert, L., Miller, J., & Barrett, A. (2014). Changes in Arctic melt season and implications for sea ice loss. *Geophysical Research Letters*, *41*, 1216–1225. https://doi.org/10.1002/2013GL058951

Suez Canal Authority (2010). Toll calculator. Retrieved from http://www.suezcanal.gov.eg/calc.aspx

Tang, Q., Zhang, X., Yang, X., & Francis, J. A. (2013). Cold winter extremes in northern continents linked to Arctic sea ice loss. *Environmental Research Letters*, *8*(1), 014036. https://doi.org/10.1088/1748-9326/8/1/014036

Transport Canada (1998). Arctic ice regime shipping system (AIRSS) standards. Ottawa.

Twomey, S. (1977). The influence of pollution on the shortwave albedo of clouds. *Journal of Atmospheric Science*, *34*(7), 1149–1152. https://doi.org/10.1175/1520-0469(1977)034<1149:TIOPOT>2.0.CO;2

Wallace, J. M., & Hobbs, P. (2006). *Atmospheric science: An introductory survey* (2nd ed.). Burlington: Academic Press.

Wang, H., Easter, R. C., Rasch, P. J., Wang, M., Liu, X., Ghan, S. J., et al. (2013). Sensitivity of remote aerosol distributions to representation of cloud–aerosol interactions in a global climate model. *Geoscientific Model Development*, *6*(3), 765–782. https://doi.org/10.5194/gmd-6-765-2013

Winiger, P., Andersson, A., Eckhardt, S., Stohl, A., Semiletov, I. P., Dudarev, O. V., et al. (2017). Siberian Arctic black carbon sources constrained by model and observation. *Proceedings of the National Academy of Sciences*, *114*(7), E1054–E1061. https://doi.org/10.1073/pnas.1613401114

Wobus, C., Flanner, M., Sarofim, M. C., Moura, M. C. P., & Smith, S. J. (2016). Future Arctic temperature change resulting from a range of aerosol emissions scenarios. *Earth's Future*, *4*(6), 270–281. https://doi.org/10.1002/2016EF000361

Yang, Y., Wang, H., Smith, S. J., Easter, R. C., & Rasch, P. J. (2018). Sulfate aerosol in the Arctic: Source attribution and radiative forcing. *Journal of Geophysical Research: Atmospheres*, *123*, 1899–1918. https://doi.org/10.1002/2017JD027298

Yumashev, D., van Hussen, K., Gille, J., & Whiteman, G. (2017). Towards a balanced view of Arctic shipping: Estimating economic impacts of emissions from increased traffic on the Northern Sea Route. *Climatic Change*, *143*(1-2), 143–155. https://doi.org/10.1007/s10584-017-1980-6

Zhou, C., & Penner, J. E. (2017). Why do general circulation models overestimate the aerosol cloud lifetime effect? A case study comparing CAM5 and a CRM. *Atmospheric Chemistry and Physics*, *17*(1), 21–29. https://doi.org/10.5194/acp-17-21-2017